Proceedings of the Seventeenth International Conference on
Civil, Structural and Environmental Engineering Computing
Edited by: P. Iványi, J. Kruis and B.H.V. Topping
Civil-Comp Conferences, Volume 6, Paper 6.1
Civil-Comp Press, Edinburgh, United Kingdom, 2023
doi: 10.4203/ccc.6.6.1

Fast stability analysis of masonry domes and vaults subjected to gravity-induced loads

D. Aita[1], G. Milani[2] and A. Taliercio[1]

[1]Department of Civil and Environmental Engineering (DICA), Politecnico di Milano, Italy
[2] Department of Architecture, Built environment and Construction engineering (ABC), Politecnico di Milano, Italy

Abstract

This paper presents two different (semi)analytical methods for the limit analysis of masonry structures, i.e., a static approach known as "stability area method", theoretically framed within the lower bound theorem of limit analysis, and a kinematic approach, based on the upper bound theorem. The analysis is conducted on case studies of masonry domes and vaults subjected to a vertical load applied at the crown. The collapse load is obtained by considering different hypotheses on the masonry tensile and compressive strengths. The results are compared with those deriving from experimental tests available in the literature.

Keywords: limit analysis, collapse load, masonry, domes, vaults

1 Introduction

In this paper, the stability analysis of masonry domes and vaults subjected to gravity-induced loads is performed by considering the self-weight and a vertical point load applied at the crown – which in domical structures corresponds to an element of architectural interest, i.e., the lantern.

Given the complex mechanical behaviour of masonry, this issue has been tackled by means of very different approaches, ranging from the implementation of Finite Element or Distinct Element codes [1,2] to numerical methods based on the Thrust Network Analysis [3,4] or homogenized limit analysis [5]. A thorough examination of the state of the art on such issue is out of the scope of this paper. The interested reader can be addressed to [6] for a more accurate overview.

The aim of this paper is to obtain fast methods to predict the bearing capacity of masonry domes and vaulted structures. To this purpose, the results obtained via two different approaches framed within the context of limit analysis are compared. The first method re-visits a classical graphical procedure [7] based on the lower bound theorem of limit analysis. The second method exploits the upper bound theorem of limit analysis and the virtual work theorem [6,8].

2 Static method

The static approach is a modern version of the stability area method, a historical procedure originally conceived for symmetric masonry arches by Durand-Claye [7] and later extended by himself, even if not entirely coherently, to masonry domes [9]. In recent years this technique has been re-visited and computerized by Aita, Barsotti and Bennati [10,11] by resulting in an effective tool for assessing the existence of statically admissible solutions in symmetric masonry structures. This method allows one to take into account strengths requirements for masonry, such as a limited compressive strength, and a limited (or nil) tensile strength. For the purposes of this contribution, an infinite friction coefficient is assumed.

As regards symmetric masonry arches, the application of the stability area method is straightforward by considering both strength limitations and equilibrium conditions of each portion of the arch comprised between the ideal vertical crown section and an arbitrary joint [10]. Conversely, in assessing the stability of domes and vaults their 3-dimensional behaviour must be considered, together with the consequences of the hypotheses on the mechanical behaviour of masonry. Namely, in masonry domes the weak tensile strength of the material causes cracking starting from the lower portion of such structures, where the hooping action vanishes as the stresses exerted along the parallels exceed the tensile strength [12]. The cracked dome can be assumed to be divided into a number of lunes behaving two by two as independent arches (Figure 1). An analogous mechanical behaviour is found in cloister vaults, where the half-arches of variable width are comprised between vertical planes passing through the diagonals of the square (or rectangular) plan (Figure 2a,b).

The starting point of the static analysis consists in imposing the equilibrium of a single lune.

In Figure 1, the scheme of two domes of revolution is shown: (*a*) is a hemispherical dome of extrados radius R and constant thickness t; (*b*) represents an ogival dome with *oculus*. In Figures 1c and 1d the plan of such domes and the corresponding subdivision into lunes is shown. In Figures 2a, 2b, the scheme of a cloister vault obtained by intersecting two identical semi-circular barrels vaults of constant thickness t, with extrados radius R, is represented. Both structures are subjected to their self-weight, with unit weight γ, and the weight of a point vertical load, λ, at the top crown.

For the domes, the amplitude of each lune is supposed to be defined by a 'small' angle $d\varphi$ (Figures 1c, 1d); for the cloister vault, the amplitude of the half-arches is equal to $\pi/2$ (Figure 2b). Since these lunes behave as one half of a symmetric arch of variable width, for each of the masonry structures represented in Figures 1 and 2a,b, the equilibrium of the lune's portion comprised between the crown and any joint, identified by the angle α shown in Figure 2c, is considered.

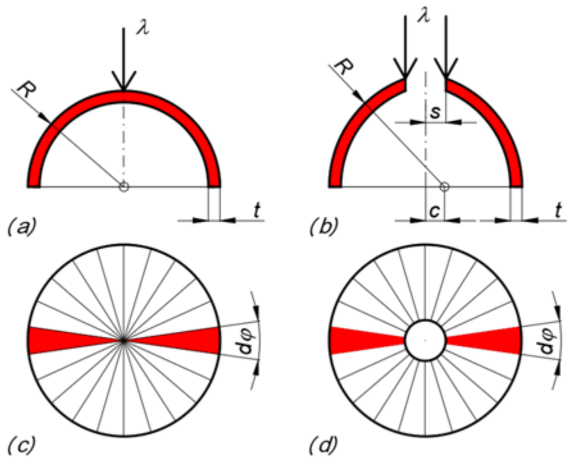

Figure 1: Scheme of masonry domes with lantern: (a) hemispherical dome; (b) ogival dome with *oculus*; (c,d) subdivision into lunes.

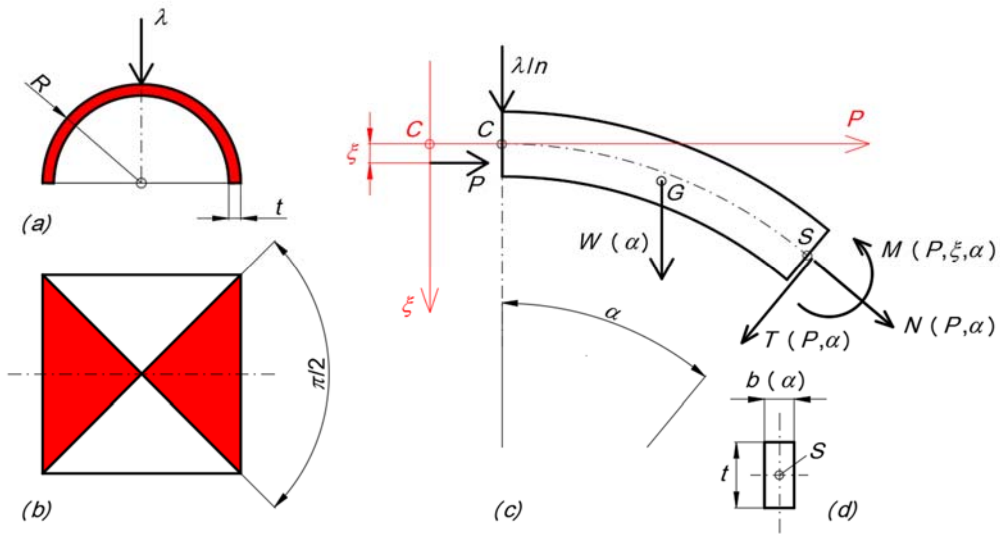

Figure 2: Scheme of cloister vault with a vertical load at the crown: (a) semicircular profile; (b) subdivision into four half-arches of variable thickness; (c) equilibrium of a *voussoir* comprised between the crown and joint α; (d) cross-section at any joint α.

In addition to the self-weight, a single lune is then subjected to a vertical crown load equal to λ/n, where $n = 2\pi/d\varphi$ for domes of revolution, $n = 4$ for cloister vaults. Because of symmetry, at the crown, a horizontal thrust, *P*, acts with an eccentricity ξ with respect to the centroid, *C*, of the ideal crown joint (Figure 2c). For domes with *oculus*, the point of application of P is referred to a given reference point. The equilibrium conditions related to the portion of the lune comprised between the ideal vertical crown section and any joint α allows one to write the formal expressions for the normal force, $N = N(\alpha, P)$, the shear force, $T = T(\alpha, P)$, and the bending moment, $M = M(\alpha, P, \xi)$ (positive if acting as shown in Figure 2c).

As regards the strength requirements, it is well known that the behaviour of masonry is very complex [12]. According to the simplifying hypotheses proposed by Heyman [13], masonry can be considered a no-tension material with infinite compressive strength. A more precise description, however, should consider its low tensile strength, f_t, and high compressive strength, f_c. If f_t and f_c are assumed to be both finite, the limit bending moment at any cross section is given by:

$$M_{lim} = \frac{(f_c\, t\, b + N)(f_t\, t\, b - N)}{2b(f_c + f_t)}, \tag{1}$$

where $N = N(\alpha, P)$ and $b = b(\alpha)$ (Figure 2d) is the width of the cross section at any joint α. More in detail, for domes of revolution, the conical surface of the joint can be approximated by a rectangle of area $t \times b$ (Figure 2d), where $b = b(\alpha) = (R - t/2)\sin\alpha\ \mathrm{d}\varphi$ for hemispherical domes (Figures 1a, 2c), $b = b(\alpha) = [(R - t/2)\sin\alpha - c]\mathrm{d}\varphi$ for ogival domes with *oculus* (Figure 1b), $b = b(\alpha) = 2(R - t/2)\sin\alpha$ for cloister vaults (Figure 2a).

At any joint α, the bending moment, $M(\alpha, P, \xi)$, is bounded by the limit value, $M_{lim} = M_{lim}(\alpha, P)$, i.e., $-M_{lim}(\alpha, P) \leq M(\alpha, P, \xi) \leq M_{lim}(\alpha, P)$.

Let us now consider the (P, ξ) plane. For any given joint α, the two curves implicitly defined by

$$M(\alpha, P, \xi) = \pm M_{lim}(\alpha, P) \tag{2}$$

identify a region, denoted by A_α, whose points (P, ξ) correspond to statically admissible solutions (i.e., fulfilling equilibrium and strength requirements) for the portion of lune comprised between the ideal vertical crown section and any joint α (Figure 3a).

The procedure described above can be repeated for all the joints along the lune. By intersecting all the $A_\alpha -$ regions, the stability area *A*, is obtained, i.e., the *locus* of all the points of coordinates (P, ξ) corresponding to statically admissible solutions in terms of crown thrust, P, and eccentricity, ξ, with respect to point C (see the green region in Figure 3a).

By considering a single lune/arch, the shape of the stability area provides a preliminary assessment of the system's stability. By adopting the strength requirements given by (1), the existence of statically admissible solutions is guaranteed if the stability area is non-vanishing (Figure 3a). These solutions correspond to an infinite set of admissible thrust lines. For a single lune, the collapse condition is found when the stability area reduces to a single point (Figure 3b). To determine the collapse load for masonry domes and cloister vaults, the procedure just described is only the first step. Indeed, the occurrence of a kinematically admissible mechanism for the entire structure has to be checked [11]. In the examples examined in this paper (see Section 4) the collapse mechanism identified when the stability area shrinks to a single point corresponds to a kinematically admissible mechanism, both for the single lune and for the entire dome/cloister vault (Figure 4).

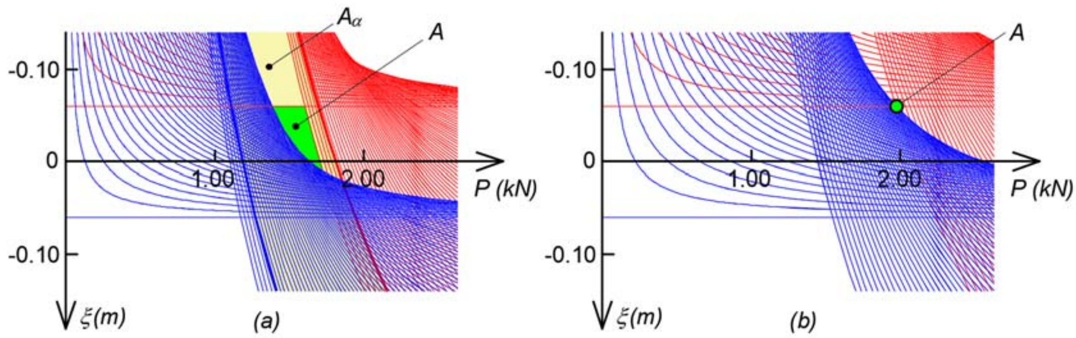

Figure 3: Stability area A related to one of the four half-arches forming a cloister vault with t = 0.12 m, R = 1 m, γ = 20 kN/m^3, f_t = 0, $f_c \to \infty$: λ = 2 kN (a); $\lambda = \lambda_{lim}$ = 3.4804 kN (b).

3 Kinematic method

In the kinematic approach, based on the principle of virtual work, a suitable mechanism is assumed *a priori*. As a starting point, such mechanism is chosen by considering the results of analytical and numerical investigations on masonry domes and vaults [6, 14], as well as the analyses carried out according to the static method described in Section 2; the analysed structures are implicitly assumed to be assemblages of rigid bodies with unilateral constraints. For the hemispherical dome of Figure 1a,c, a kinematically admissible mechanism characterized by the occurrence of three annular flexural hinges is assumed, namely, an extrados hinge at the crown, an intrados hinge at an intermediate joint α_H, and an extrados hinge at the base of the dome (Figure 4a). For the cloister vault of Figure 2a,b, an analogous mechanism is considered, with three cylindrical flexural hinges (Figure 4b).

The procedure is described in detail in [6], to which interested readers are referred. For the purposes of this contribution, it is sufficient to briefly recall the main steps.

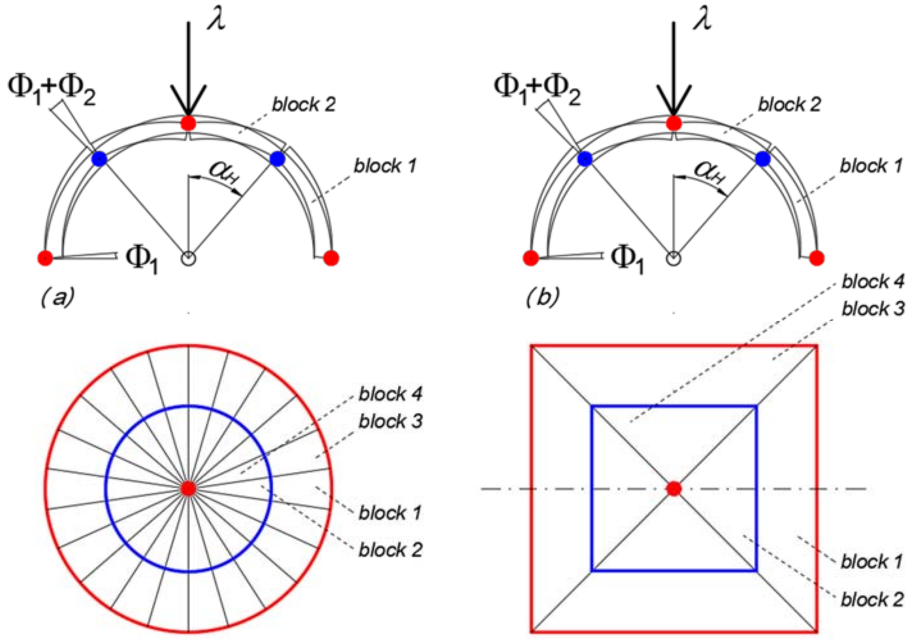

Figure 4: Kinematically admissible mechanism
for a masonry dome (a) and for a cloister vault (b).

Referring to the pre-selected mechanism, let Φ_1 denote the rotation rate of the hinge at the base of the dome/vault and $\Phi_1 + \Phi_2$ the rotation rate of the intermediate hinge, α_H (Figure 4). The interfaces on a meridian between two contiguous lunes (in masonry domes) and those on the diagonal arches (in cloister vaults) are exclusively subjected to a jump in normal velocity, which can be expressed in terms of Φ_1 and Φ_2.

The internal power P_d dissipated on the meridional or diagonal interfaces can then be expressed in closed form as the sum of that between blocks 1 and 3 and that between blocks 2 and 4 (Figure 4), by considering the ultimate tensile strength of the vault along the meridian/diagonal arches, f_{td}. Then, the power P_w done by the dome/vault self-weight is evaluated, after analytically determining the location of the centroids of blocks 1 and 2 (Figure 4). Finally, the dissipation P_h along the horizontal hinges at joint α_H and at the base, is analytically determined by taking into account the ultimate tensile strength, f_t, along these hinges.

The kinematic collapse load can be therefore expressed in closed form:

$$\lambda = n\frac{P_h + P_d - P_w}{x_{C_2}\Phi_2}, \tag{3}$$

where x_{C_2} is the horizontal distance between the instant rotation center C_2 and the vertical straight line passing through the crown (Figure 5a); $n = 2\pi/d\varphi$ for the dome of revolution, $n = 4$ for the cloister vault.

The position of joint α_H is univocally identified by minimizing the kinematic collapse load, λ.

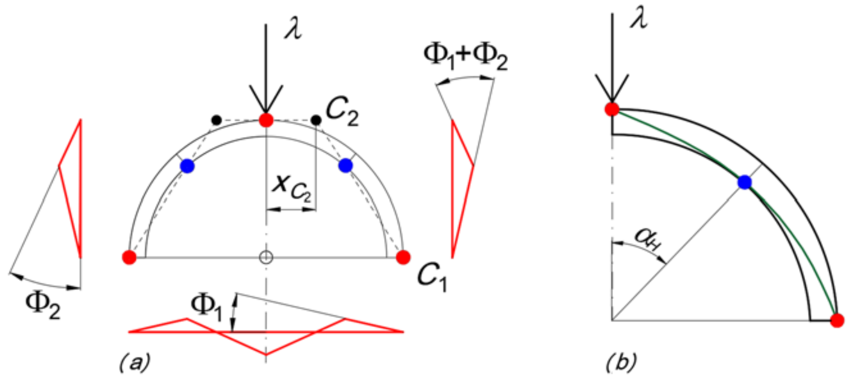

Figure 5: (a) Kinematic chain and location of the instant centers of rotation; (b) thrust line corresponding to the collapse load (cloister vault with $t = 0.12$ m, $R = 1$ m, $\gamma = 20$ kN/m^3, $f_t = 0$, $f_c \rightarrow \infty$; $\lambda = \lambda_{lim} = 3.4804$ kN).

4 Results

The static and kinematic approaches described in Sections 2 and 3 are now applied to two vaulted masonry structures experimentally tested: a hemispherical dome and a cloister vault with *radius* $R = 1$ m, thickness $t = 0.12$ m, and unit weight $\gamma = 20\,\mathrm{kN/m^3}$ (see Figure 1a,c; Figure 2a,b) [15, 16]. The mechanical behaviour of these structures has been studied in [6, 17], providing useful material for a suitable comparison between different methods.

The collapse load can be obtained through the static method by drawing the *stability area* in the (P, ξ) plane. The analysis is performed by subdividing the dome into 360 lunes of amplitude $d\varphi = 1°$, whereas the cloister vault is subdivided in four half-arches of amplitude $\pi/2$. In turn, each lune is subdivided in 90 blocks.

Regarding the tensile and compressive strength, four different hypotheses on the masonry mechanical behaviour are considered:

(a) $f_t = 0.05$ MPa, $f_c = 2.2$ MPa;
(b) $f_t = 0.05$ MPa, $f_c \rightarrow \infty$;
(c) $f_t = 0$, $f_c = 2.2$ MPa;
(d) $f_t = 0$, $f_c \rightarrow \infty$.

The static collapse load, for each of these cases, is obtained by progressively increasing the value of λ, until a threshold value, λ_{lim}, is reached as the stability area vanishes. As an example, in Figure 3b the stability area corresponding to the collapse load for the cloister vault under examination is plotted, by assuming $f_t = 0$, $f_c \rightarrow \infty$. The limit value is $\lambda = \lambda_{lim} = 3.4804$ kN.

As can be seen from the outcomes related to the dome (Table 1) and to the cloister vault (Table 2), the value of λ_{lim} is extremely sensitive to the value of the tensile strength, however low. For the cases corresponding to a limited compressive strength, identified in Table 1 and Table 2 with an asterisk (*), the crown hinge is assumed to be defined by angle $\alpha = 1°$, since the area of the cross section would vanish at $\alpha = 0°$ and a singularity in the bending moment capacity at this section would occur.

Table 1. The collapse load, λ_{lim}, for the benchmark dome ($R = 1$ *m*, $t = 0.12$ *m*).

Masonry strength	*Collapse load,* λ_{lim}	*Intermediate hinge location,* α_H
$f_t = 0.05$ MPa, $f_c = 2.2$ MPa*	8.892 kN	27°
$f_t = 0.05$ MPa, $f_c \rightarrow \infty$	10.748 kN	31°
$f_t = 0$, $f_c = 2.2$ MPa*	2.599 kN	41°
$f_t = 0$, $f_c \rightarrow \infty$	2.7336 kN	42°

Table 2. The collapse load, λ_{lim}, for the benchmark cloister vault ($R = 1$ *m*, $t = 0.12$ *m*).

Masonry strength	*Collapse load,* λ_{lim}	*Intermediate hinge location,* α_H
$f_t = 0.05$ MPa, $f_c = 2.2$ MPa*	11.321 kN	28°
$f_t = 0.05$ MPa, $f_c \rightarrow \infty$	13.688 kN	31°
$f_t = 0$, $f_c = 2.2$ MPa*	3.3081 kN	42°
$f_t = 0$, $f_c \rightarrow \infty$	3.4804 kN	42°

As an example, in Figure 5b the thrust line related to one of the four half-arches composing the cloister vault is shown. This line corresponds to the stability area plotted in Figure 3b ($t = 0.12$ m, $R = 1$ m, $\gamma = 20$ kN/m^3, $f_t = 0$, $f_c \rightarrow \infty$), obtained at the collapse load, $\lambda = \lambda_{lim} = 3.4804$ kN. The position of the hinges, i.e., the joints where the bending moment attains its limit value, identifies a kinematically admissible collapse mechanism both for the half-arch and for the entire cloister vault.

In [6] the kinematic method is applied by assuming $f_t = 0.05$ MPa, $f_c \rightarrow \infty$; moreover, different values of the tensile strength along the meridian/diagonal arches, f_{td}, are assumed. The results show that the collapse load is strongly affected by the strength along the meridian/diagonal arches. The best fitting with the experimental results is obtained by setting $f_{td} = 0.08$ MPa for the dome ($\lambda_{lim} = 52.1458$ kN) and $f_{td} = 0.025$ MPa for the cloister vault ($\lambda_{lim} = 30.6504$ kN).

The results obtained through the two approaches by assuming the strength values compatible with both methods ($f_{td} = 0$, $f_t = 0$, $f_c \rightarrow \infty$ and $f_{td} = 0$, $f_t = 0.05$ MPa, $f_c \rightarrow \infty$) are in good agreement.

5 Conclusions and Contributions

Assessing the load bearing capacity of masonry domes and vaults subjected to gravity-induced loads is not an easy task. This contribution aims at developing two (semi)analytical methods based either on the static or the kinematic theorem of limit analysis, which provide safe and unsafe approximations of the collapse load by enriching Heyman's hypotheses. In the static approach a limited tensile and compressive strength along the joints can be taken into account, whereas in the kinematic approach the tensile strength both along the joints and along the meridian/diagonal arches can be incorporated.

The (semi)analytical solutions are of technical interest since the load bearing capacity of the considered masonry structures can be evaluated in closed form, without resorting to numerical methods. Moreover, both methods can be easily adapted to different geometries and load conditions.

In the continuation of the research, the proposed methods will be applied to some interesting case studies belonging to the architectural heritage. As an example, the dome of the Church of *Anime Sante* in L'Aquila (Italy) and the dome of *Escuelas Pías* in Valencia (Spain) both match the scheme shown in Figures 1b,d including an *oculus*. Another interesting case study that can be analysed by the proposed approach is represented by the *Global Vipassana Pagoda*, the world's largest span stone masonry dome (Mumbai, India), consisting in a hemispherical dome with a small *oculus* and a conical lantern.

References

[1] G. Milani, A. Tralli, "A simple meso-macro model based on SQP for the non-linear analysis of masonry double curvature structures", International Journal of Solids and Structures, 49, 808-834, 2012.

[2] G. Lengyel, K. Bagi, "Horizontal reaction components of pointed vaults", International Journal of Masonry Research and Innovation, 1(4), 398-420, 2016.

[3] P. Block, J. Ochsendorf, "Thrust Network Analysis: A new methodology for three-dimensional equilibrium", Journal of The International Association for Shell and Spatial Structures, 48 (3), 167-173, 2007.

[4] M. Bruggi, "A constrained force density method for the funicular analysis and design of arches, domes and vaults", International Journal of Solids and Structures, 193-194, 251-269, 2020.

[5] G. Milani, "Upper bound sequential linear programming mesh adaptation scheme for collapse analysis of masonry vaults", Advances in Engineering Software, 79, 91-110, 2015.

[6] G. Milani, "Closed form solutions in Limit Analysis for masonry cloister vaults and domes subjected to concentrated vertical loads applied at the top crown", International Journal of Masonry Research and Innovation, in press.

[7] A. Durand-Claye, "Note sur la vérification de la stabilité des voûtes en maçonnerie et sur l'emploi des courbes de pression", Annales des Ponts et Chaussées, 13: 63-93, 1867.

[8] A. Sinopoli, M. Corradi, F. Foce, "Modern formulation for preelastic theories on masonry arches", Journal of Engineering Mechanics, ASCE, 123(3), 204-213, 1997.

[9] A. Durand-Claye, "Vérification de la stabilité des voûtes et des arcs: applications aux voûtes sphériques", Annales des Ponts et Chaussées, 19(1), 416-440, 1880.

[10] D. Aita, R. Barsotti, S. Bennati, "Looking at the collapse modes of circular and pointed masonry arches through the lens of Durand-Claye's stability area method", Archive of Applied Mechanics, 89, 1537-1554. 2019.

[11] D. Aita, R. Barsotti, S. Bennati, "Studying the dome of Pisa cathedral via a modern reinterpretation of Durand-Claye's method", Journal of Mechanics of Materials and Structures, 14(5), 603-619, 2019.

[12] A.M. D'Altri, V. Sarhosis, G. Milani, J. Rots, S. Cattari, S. Lagomarsino, E. Sacco, A. Tralli, G. Castellazzi, S. de Miranda, "Modeling strategies for the computational analysis of unreinforced masonry structures: Review and classification", Archives of Computational Methods in Engineering, 27(4), 1153-1185, 2020.

[13] J. Heyman, The stone skeleton, International Journal of Solids and Structures, 2(2), 249-279, 1966.

[14] A. Chiozzi, G. Milani, A. Tralli, "A Genetic Algorithm NURBS-based new approach for fast kinematic limit analysis of masonry vaults", Computers and Structures, 182, 187-204, 2017.

[15] P. Faccio, P. Foraboschi, E. Siviero, "Volte in muratura con rinforzi in FRP". L'Edilizia, 7/8, 44-58, 1999.

[16] P. Foraboschi, "Strengthening of Masonry Arches with Fiber-Reinforced Polymer Strips", Journal of Composites for Construction, ASCE, 8(3), 191-202, 2004.

[17] E. Milani, G. Milani, A. Tralli, "Limit analysis of masonry vaults by means of curved shell finite elements and homogenization", International Journal of Solids and Structures, 45, 5258-5288, 2008.